Human Molecular Genetics, 2009, Vol. 18, No. 2 ***227–240***
doi:10.1093/hmg/ddn339
Advance Access published on October 15, 2008

FGFR3 promotes synchondrosis closure and fusion of ossification centers through the MAPK pathway

Takehiko Matsushita[1], William R. Wilcox[3,4], Yuk Yu Chan[1], Aya Kawanami[1], Hülya Bükülmez[2,5], Gener Balmes[6], Pavel Krejci[3,7,8], Pertchoui B. Mekikian[3], Kazuyuki Otani[9], Isakichi Yamaura[9], Matthew L. Warman[10], David Givol[11] and Shunichi Murakami[1,2,*]

[1]Department of Orthopaedics and [2]Department of Genetics, Case Western Reserve University, 10900 Euclid Avenue, Cleveland, OH 44106, USA, [3]Medical Genetics Institute, Cedars-Sinai Medical Center, 8700 Beverly Blvd, Los Angeles, CA 90048, USA, [4]Department of Pediatrics, UCLA School of Medicine, Los Angeles, CA 90095, USA, [5]Department of Pediatrics, Pediatric Rheumatology, MetroHealth Medical Center, 2500 MetroHealth Drive, Cleveland, OH 44109, USA, [6]Department of Molecular Genetics, University of Texas M.D. Anderson Cancer Center, 1515 Holcombe Blvd, Houston, TX 77030, USA, [7]Institute of Experimental Biology, Masaryk University 61137, Brno, Czech Republic, [8]Department of Cytokinetics, Institute of Biophysics ASCR 61265, Brno, Czech Republic, [9]Department of Orthopaedic Surgery, Kudanzaka Hospital, 2-1-39 Kudanzakaminami, Chiyoda-ku, Tokyo 102-0071, Japan, [10]Department of Orthopaedic Surgery, and the Howard Hughes Medical Institute at Children's Hospital, Boston, 300 Longwood Avenue, Boston, MA 02115, USA and [11]Weizmann Institute of Science, Rehovot, Israel 76100

Received July 9, 2008; Revised October 6, 2008; Accepted October 13, 2008

Activating mutations in FGFR3 cause achondroplasia and thanatophoric dysplasia, the most common human skeletal dysplasias. In these disorders, spinal canal and foramen magnum stenosis can cause serious neurologic complications. Here, we provide evidence that FGFR3 and MAPK signaling in chondrocytes promote synchondrosis closure and fusion of ossification centers. We observed premature synchondrosis closure in the spine and cranial base in human cases of homozygous achondroplasia and thanatophoric dysplasia as well as in mouse models of achondroplasia. In both species, premature synchondrosis closure was associated with increased bone formation. Chondrocyte-specific activation of Fgfr3 in mice induced premature synchondrosis closure and enhanced osteoblast differentiation around synchondroses. FGF signaling in chondrocytes increases Bmp ligand mRNA expression and decreases Bmp antagonist mRNA expression in a MAPK-dependent manner, suggesting a role for Bmp signaling in the increased bone formation. The enhanced bone formation would accelerate the fusion of ossification centers and limit the endochondral bone growth. Spinal canal and foramen magnum stenosis in heterozygous achondroplasia patients, therefore, may occur through premature synchondrosis closure. If this is the case, then any growth-promoting treatment for these complications of achondroplasia must precede the timing of the synchondrosis closure.

INTRODUCTION

Longitudinal bone growth occurs through endochondral ossification, in which chondrocytes progress through a series of proliferation and differentiation processes. Chondrocytes in the reserve zone of growth plates proliferate and then exit the cell cycle to differentiate into hypertrophic chondrocytes. The increase in the number of chondrocytes by proliferation, the increase in the size of chondrocytes by hypertrophy and the synthesis of extracellular matrix all contribute to linear growth. Chondrocytes in growth plates are continuously supplied by the differentiation and proliferation of chondrocytes in the reserve and proliferative zones, while terminally differentiated hypertrophic chondrocytes are removed at the chondro-osseous junction by apoptotic cell death. The balance between the addition and removal of chondrocytes

*To whom correspondence should be addressed at: Dept of Orthopaedics, Case Western Reserve University, 2109 Adelbert Road, BRB 329, Cleveland, OH 44106, USA. Tel: +1 2163681371; Fax: +1 2163681332; Email: shun@case.edu

as well as matrix production and degradation determines the height of the growth plates. In humans, the cessation of linear growth usually coincides with the end of puberty when growth plates become entirely replaced by bone.

Similar to the appendicular skeleton, in the vertebrae, sternum and cranial base, bone growth occurs at synchondroses—cartilaginous structures consisting of two opposed growth plates with a common zone of resting chondrocytes. As with endochondral growth plates, synchondroses also become replaced by bone. The regulation of growth plate and synchondrosis closure is still not entirely understood.

Endochondral ossification is controlled by multiple regulatory factors (1,2). An essential regulator of endochondral bone growth is fibroblast growth factor receptor 3 (Fgfr3). *Fgfr3* is preferentially expressed in proliferating and prehypertrophic chondrocytes in epiphyseal growth plates (3,4). Activating mutations in FGFR3 cause autosomal dominant human skeletal disorders, achondroplasia, thanatophoric dysplasia and hypochondroplasia (5–9). Thanatophoric dysplasia is the most common lethal skeletal dysplasia, and achondroplasia is the most common non-lethal form of dwarfism. Despite its non-lethality, common and serious complications in achondroplasia are a small foramen magnum and spinal stenosis (10,11) (Fig. 1). Stenosis of the foramen magnum, the orifice in the occipital bone through which passes the spinal cord from the medulla oblongata, has been associated with hydrocephalus and sudden death in infancy (12–14) as well as headaches in older children (15). Currently, surgical enlargement of very small foramen magnum is recommended for $<10\%$ of children with achondroplasia (11,16). Narrowing of the spinal canal, which contains the spinal cord and cauda equina, is a common complication in adults with achondroplasia and can cause neurologic deficits including myelopathy, radiculopathy and neurogenic claudication. In addition, insufficient growth of the cranial base causes midface hypoplasia, which leads to obstructive sleep apnea, otitis media and dental malocclusion.

Inadequate growth of the spinal canal, foramen magnum and cranial base in patients with FGFR3 mutations could be due to deficient cell proliferation, hypertrophy and/or matrix production, and/or due to premature closure of synchondroses. Support for the latter mechanism comes from computed tomography (CT) studies in patients with achondroplasia where premature closure of occipital bone synchondroses was observed (17). To explore the developmental mechanisms that contribute to these complications, we examined synchondroses of the spine and cranial base in human specimens from children who died from homozygous achondroplasia and thanatophoric dysplasia, and we studied the timing of synchondrosis closure in mice with the Fgfr3 mutation G374R, which corresponds to the common human achondroplasia mutation, and in mice that express a constitutively active form of MEK1, a downstream effector of Fgfr3 signaling. In humans and in mice, we observed premature closure of multiple synchondroses. Our results indicate that Fgfr3 and MAPK signaling in chondrocytes regulate synchondrosis closure, osteoblast differentiation and bone formation, providing novel insights into the developmental mechanisms of spinal canal stenosis, foramen magnum stenosis and midface hypoplasia in achondroplasia. If premature synchondrosis closure accounts for spinal canal stenosis, foramen magnum stenosis and midface hypoplasia, then future growth-promoting treatment for these complications must start before the synchondroses close.

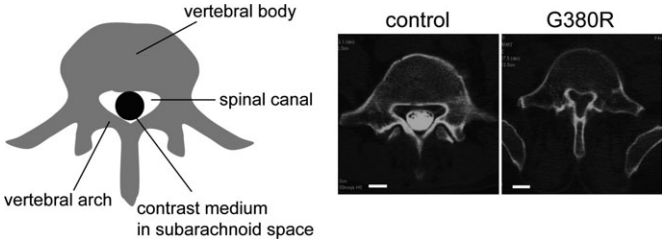

Figure 1. Spinal canal stenosis in achondroplasia. Axial CT myelogram of the fifth lumbar spine shows the narrowing of the spinal canal in a 46-year-old female achondroplasia patient with FGFR3 G380R mutation, who presented with paraparesis (right). The contrast medium injected into the subarachnoid space was excluded in the achondroplasia patient due to severe spinal canal stenosis. (Left) 41-year-old female patient with irrelevant spinal disorder. White bars indicate 1 cm.

RESULTS

Human specimens from homozygous achondroplasia and thanatophoric dysplasia were examined at the International Skeletal Dysplasia Registry at Cedars-Sinai Medical Center. The synchondroses in the cranial base and lumbar vertebrae were examined in one case of homozygous achondroplasia, four cases of thanatophoric dysplasia (three perinatal, one fetal) and one control fetus (Table 1).

Premature synchondrosis closure in homozygous achondroplasia

Gross inspection and radiographic examination of the mid-sagittal slice of the cranial base in an infant who died from homozygous achondroplasia (Case 1) showed absence or premature closure of the spheno-occipital synchondrosis (Fig. 2B and C), which normally closes between 11 and 25 years of age (18–22). We also examined the neurocentral synchondroses of the lumbar vertebrae that normally close between 3 and 14 years of age (23–26). X-ray examination of the third lumbar spine showed complete fusion of the neurocentral synchondrosis on one side and partial fusion on the other side (Fig. 2D), consistent with premature closure. Fusion was confirmed histologically (data not shown).

Premature synchondrosis closure in thanatophoric dysplasia

We also examined one 27-week thanatophoric dysplasia fetus with an R248C mutation (Case 2) and one 26-week gestation control without any signs of skeletal dysplasia (Case 3). Radiographic examination showed narrowing of the foramen magnum in the thanatophoric dysplasia fetus (Fig. 2E and F). Although the intraoccipital synchondroses were still open at this stage, this fetus had a bony bridge forming around the anterior intraoccipital synchondroses (Fig. 2E) that was

Table 1. Summary of human samples of homozygous achondroplasia and thanatophoric dysplasia

Case			Mutation	Age	Neurocentral (lumbar spine)	Spheno-occipital	Anterior intraoccipital
1	Homozygous ACH	R73-70B	G380R	Neonatal	L3 closed	Closed	Not examined
2	TDI	R01-270	R248C	27 weeks gestation	Not examined	Open	Open
3	control	93-21		26 weeks gestation	Not examined	Open	Open
4	TDI	R98-179	X807S	5 days	L1, L2 closed	Not examined	Partially closed
5	TDI	R99-512	R248C	36 weeks gestation	Not examined	Partially closed	Partially closed
6	TDI	R98-383	R248C	36 weeks gestation	L1 partially closed	Partially closed	Partially closed

Synchondrosis closure was evaluated by X-ray and histology.
ACH, achondroplasia; TD I, thanatophoric dysplasia type I.

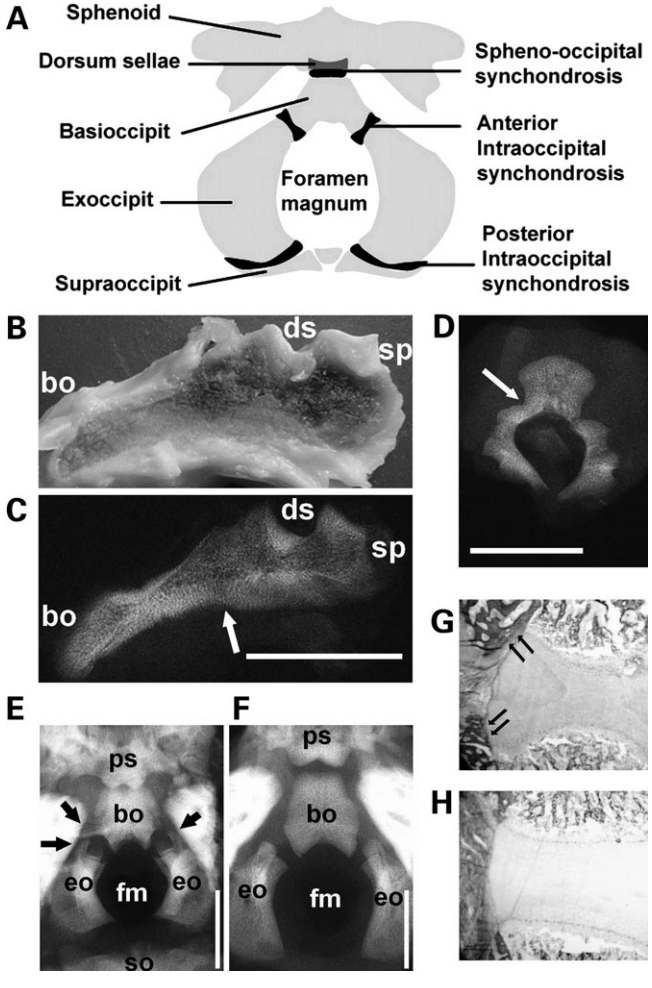

Figure 2. The spine and cranial base of homozygous achondroplasia and thanatophoric dysplasia. (**A**) An illustration of the anatomy of the cranial base. (**B**–**D**) Cranial base and lumbar spine of homozygous achondroplasia (Case 1). Gross appearance (B) and X-ray (C) of mid-sagittal slice of the cranial base of homozygous achondroplasia. Arrow indicates the fused spheno-occipital synchondrosis. (D) The third lumbar spine showed complete fusion of the neurocentral synchondrosis on one side and partial fusion on the other side. (**E** and **F**) Cranial view of the cranial base of a thanatophoric dysplasia fetus (E) (Case 2) at 27 weeks of gestation and a control fetus (F) (Case 3) at 26 weeks of gestation without any signs of skeletal dysplasia. The anterior intraoccipital synchondroses of the thanatophoric dysplasia fetus are being encased in bone (arrows). (**G** and **H**) Goldner staining of the spheno-occipital synchondrosis of Case 2 (G) and Case 3 (H), showing increased bone formation in thanatophoric dysplasia (arrows). Scale bars indicate 10 mm. Abbreviations: bo, basioccipital; eo, exoccipital; fm, foramen magnum; so, supraoccipital; sp, sphenoid; ds, dorsum sellae; ps, postsphenoid.

confirmed histologically (Fig. 2G). In contrast, no bridging bones were observed in the control fetus (Fig. 2F and H).

We also examined perinatal specimens from three neonates with thanatophoric dysplasia (Cases 4–6). Case 4 had a previously unreported G to C mutation in the stop codon, which is predicted to change the stop codon to serine residue. Cases 5 and 6 had an R248C mutation. In all cases, we observed premature closure of the cranial base and neurocentral synchondroses in association with increased bone formation (Supplementary Material, Fig. S1). Collectively, these observations indicate that activating mutations in FGFR3 cause premature synchondrosis closure and increased bone formation.

Premature synchondrosis closure in mice that express an achondroplasia mutation

To examine the role of Fgfr3 in synchondrosis closure, we analyzed a mouse knock in model of achondroplasia (27). The Fgfr3 G374R mutation corresponds to the most common human achondroplasia mutation, FGFR3 G380R. The targeted allele is a hypomorph until Cre-recombinase excises the floxed neomycin selection cassette, at which point its expression normalizes. The use of *Zp3-Cre* transgenic mice, which express Cre in oocytes, produces a normally expressed Fgfr3 G374R allele and results in dwarfism.

We found that multiple synchondroses close prematurely in mice heterozygous for the mutant Fgfr3 G374R allele ($Fgfr3^{G374R/+}$). Skeletal preparation of 10-day-old mice showed premature closure of the intersphenoid, spheno-occipital and anterior intraoccipital synchondroses in the cranial base, while corresponding synchondroses remained cartilaginous in wild-type littermates (Fig. 3A). Consistently, neurocentral synchondroses in the cervical, thoracic and lumber spine prematurely closed in $Fgfr3^{G374R/+}$ mice (Fig. 3B). The premature closure of synchondroses was also observed in the triradiate cartilage of pelvis, sternum and hyoid (Supplementary Material, Fig. S2).

Histological analyses of the premature synchondrosis closure

We first examined *Fgfr3* expression in synchondroses by *in situ* hybridization. Relatively strong expression of *Fgfr3* was observed in chondrocytes of the proliferating and prehypertrophic zones of synchondroses in the cranial base, spine and

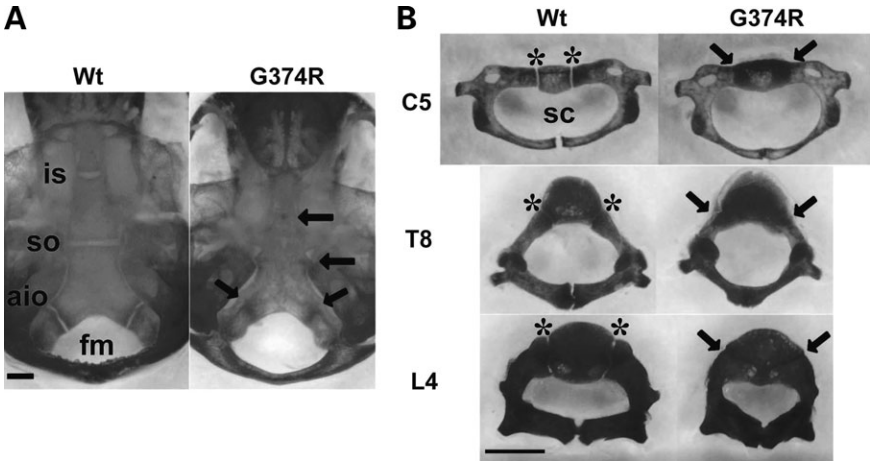

Figure 3. Skeletal preparations after alizarin red staining of mice that express Fgfr3 G374R and wild-type littermate mice at P10. Synchondroses in the cranial base (**A**) and spine (**B**) were prematurely closed in mice that express Fgfr3 G374R. Arrows indicate fused synchondroses. Asterisks indicate the neurocentral synchondroses. Scale bars indicate 1 mm. Abbreviations: Wt, wild-type mice, (G374R) mice that express Fgfr3 G374R; is, intersphenoid; so, spheno-occipital; aio, anterior intraoccipital; sc, spinal canal; C5, 5th cervical vertebrae; T8, eighth thoracic vertebrae; L4, fourth lumbar vertebrae.

sternum (Fig. 4C and data not shown). *Fgfr3* was also weakly expressed in chondrocytes of the resting zone of the synchondroses and some of the cells in the periosteum and bone spongiosa. To examine the mechanism of premature synchondrosis closure in $Fgfr3^{G374R/+}$ mice, we analyzed a series of vertebral synchondroses harvested at various stages of development. At embryonic day 16.5 (E16.5), no obvious difference was observed between wild-type embryos and $Fgfr3^{G374R/+}$ embryos (Fig. 4A). However, from postnatal day 1 (P1), the neurocentral synchondroses narrowed progressively in $Fgfr3^{G374R/+}$ mice. While the neurocentral synchondroses of wild-type mice did not close until about P14 (data not shown), neurocentral synchondroses in $Fgfr3^{G374R/+}$ mice showed partial closure at P4 and complete closure by P8. Interestingly, the growth plate-like structure of the neurocentral synchondrosis consisting of the zones of the resting, proliferating and hypertrophic chondrocytes was well maintained at P8 in wild-type mice (Fig. 4B). In contrast, $Fgfr3^{G374R/+}$ mice had premature loss of the zones of the resting and proliferating chondrocytes beginning at P2. By P4, most of the chondrocytes became hypertrophic as evidenced by immunohistochemistry for type X collagen (Fig. 4D).

Because reduced cell proliferation, early apoptosis or precocious terminal differentiation could each be responsible for the precocious synchondrosis closure, we examined proliferation of chondrocytes in the synchondrosis by bromodeoxyuridine (BrdU) incorporation, differentiation of chondrocytes by immunohistochemistry for type X collagen and apoptosis by TUNEL assay. We also looked for evidence of vascular and osteoclast/chondroclast invasion by immunohistochemistry for von Willebrand factor, MMP9, MMP13, tartrate-resistant acid phosphatase (TRAP) and *in situ* hybridization for *Vegf*. At E16.5, there was no difference in the number of BrdU-labeled cells in the neurocentral synchondrosis between wild-type and mutant mice (Fig. 4E). However, by P2, the mutant mice had fewer BrdU-labeled cells. In the wild-type synchondrosis, numerous BrdU-labeled cells were found in the zones that correspond to the proliferative zone of growth plate, while only a few chondrocytes were labeled with BrdU in the synchondrosis of $Fgfr3^{G374R/+}$ mice. Immunohistochemistry for an endothelial marker, von Willebrand factor, showed increased vascular endothelial cells at the chondro-osseous junction of synchondroses of $Fgfr3^{G374R/+}$ mice, suggesting increased vascular invasion (Fig. 4F). *In situ* hybridization analysis showed increased *Vegf* expression in hypertrophic chondrocytes of $Fgfr3^{G374R/+}$ mice compared with wild-type mice, suggesting a role for VEGF in the increased vascularization (Fig. 4G). No obvious difference was found in the number of osteoclasts/chondroclasts, apoptosis in synchondroses by TUNEL staining and expression of MMP9 and MMP13 between $Fgfr3^{G374R/+}$ mice and wild-type littermate mice in these analyses (data not shown).

Increased bone formation in the perichondrium of mice that express Fgfr3 G374R

Similar to synchondroses in humans with thanatophoric dysplasia and homozygous achondroplasia, $Fgfr3^{G374R/+}$ mice had bone formation encasing the closing synchondroses. To examine osteoblast differentiation around the closing synchondroses, we expressed the *Col1a1-LacZ* transgene in $Fgfr3^{G374R/+}$ mice. The *Col1a1-LacZ* transgene expresses *LacZ* under the control of a 2.3 kb osteoblast-specific promoter of *Col1a1*, a gene for type I collagen (28). The neomycin cassette was removed by using the *Zp3-Cre* transgene, so that the *Fgfr3* allele was recombined in a systemic fashion. X-gal staining of $Fgfr3^{G374R/+}$;*Col1a1-LacZ* mice showed a marked increase in osteoblasts around the synchondroses at P3 (Fig. 5A). We also examined the expression of Runx2, a transcription factor essential for osteoblast differentiation (29,30). Runx2-positive cells were increased in the periosteum of mutant mice compared with wild-type mice at P4 (Fig. 5B). These observations strongly suggest that increased Fgfr3 signaling promotes osteoblast differentiation around the closing synchondroses.

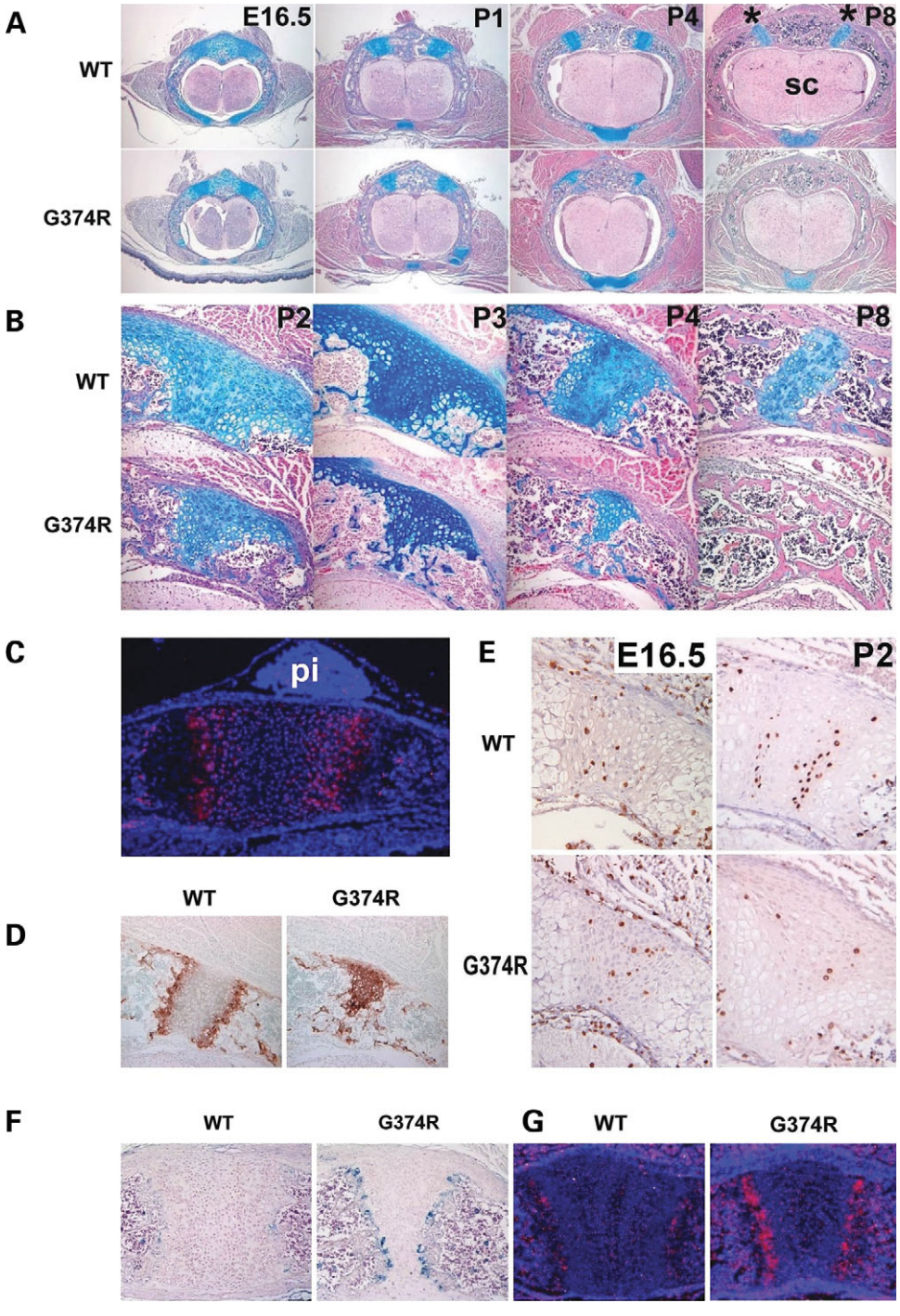

Figure 4. Premature loss of proliferating chondrocytes and increased vascular invasion in the synchondroses of mice that express Fgfr3 G374R. (**A**) Hematoxylin, eosin and alcian blue-stained horizontal sections of the spine showed premature closure of the neurocentral synchondroses in mice that express Fgfr3 G374R. Asterisk indicates neurocentral synchondroses and sc denotes spinal cord. (**B**) Higher magnification of the closing neurocentral synchondroses between P2 and P8. All the vertebrae shown in (A) and (B) are either T12 or L1. (**C**) *In situ* hybridization of *Fgfr3* of the spheno-occipital synchondrosis of wild-type mice at P1. *Fgfr3* is strongly expressed in chondrocytes in the proliferating and prehypertrophic zones. pi denotes pituitary glands. (**D**) Type X collagen immunostaining of neurocentral synchondrosis of mice that express Fgfr3 G374R and wild-type littermate mice at P4. Mice that express Fgfr3 G374R showed premature loss of the zones of resting and proliferating chondrocytes. (**E**) Immunostaining of the neurocentral synchondrosis for BrdU at E16.5 and P2. BrdU-labeled chondrocytes are markedly reduced in the closing neurocentral synchondrosis of mice that express Fgfr3 G374R at P2. (**F**) Immunostaining for von Willebrand factor showed increased vascular endothelial cells at the chondro-osseous junction of the sternum of mice that express Fgfr3 G374R at P5. (**G**) *In situ* hybridization analysis showed increased *Vegf* expression in the synchondroses of the sternum of mice that express Fgfr3 G374R at P1.

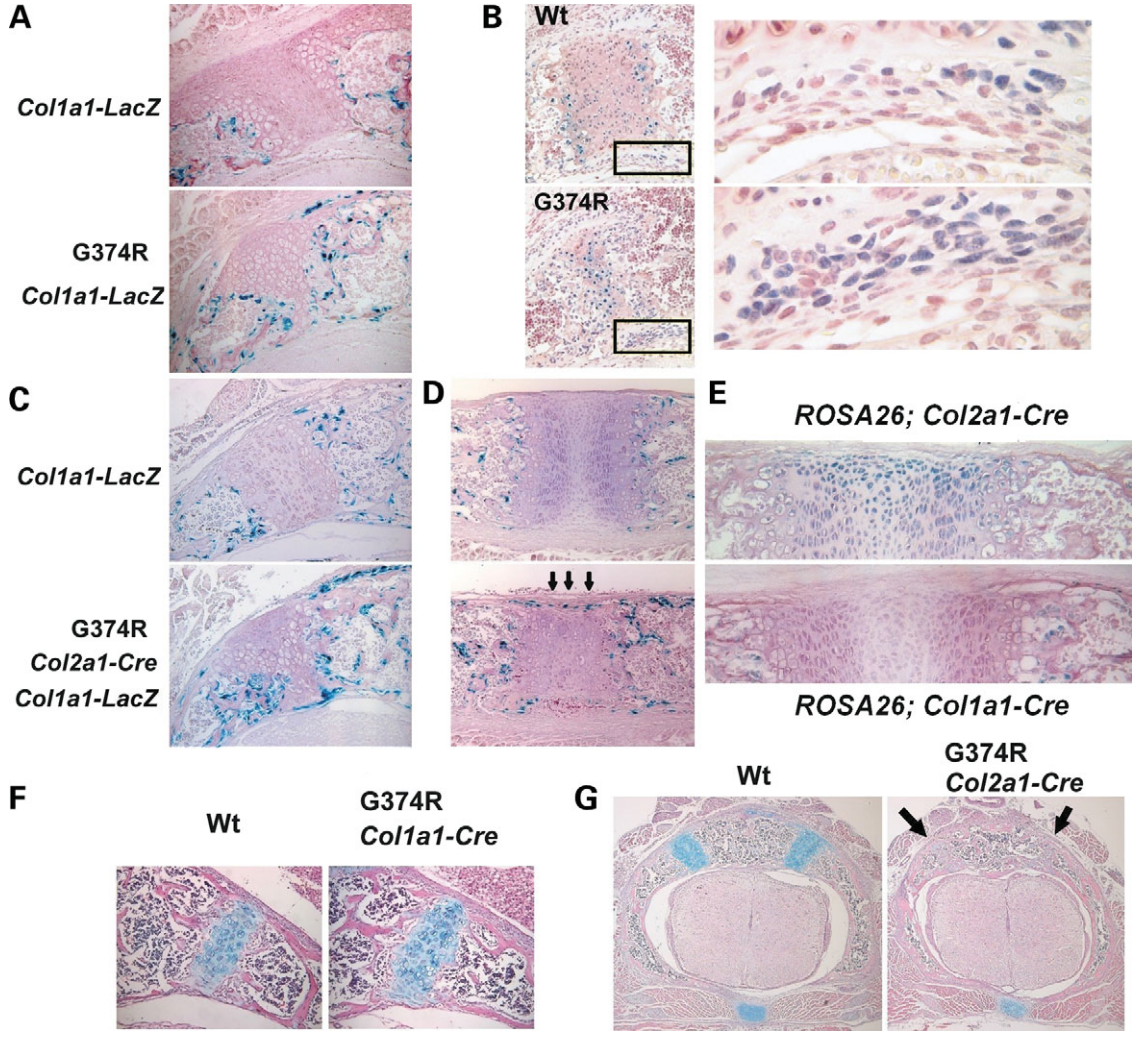

Figure 5. Increased osteoblast differentiation and bone formation in mice that express Fgfr3 G374R. (**A**) Increased number of X-gal-stained osteoblasts around the neurocentral synchondroses of the lower thoracic spine in Fgfr3 G374R mice at P3. *Zp3-Cre* transgene was used to express Fgfr3 G374R in a systemic manner. *Col1a1-LacZ* transgene was used to express *LacZ* in osteoblasts. (**B**) Immunohistochemistry for Runx2 showed an increase in Runx2-positive cells in the periosteum flanking the neurocentral synchondroses of Fgfr3 G374R mice at P4. Right panels show magnified images of the boxed areas in the left panels. (**C** and **D**) X-gal staining of the neurocentral synchondroses of the lower thoracic spine (C) and sternum (D) at P3. *Col2a1-Cre* transgene was used to express Fgfr3 G374R in chondrocytes of *Col1a1-LacZ* transgenic mice. (**E**) Chondrocyte and osteoblast-specific recombination was confirmed by crossing *Col2a1-Cre* and *Col1a1-Cre* transgenic mice with the *ROSA26* reporter mice. X-gal staining of the sternum showed chondrocyte-specific recombination by the *Col2a1-Cre* transgene at P2 and osteoblast-specific recombination by the *Col1a1-Cre* transgene at P3. (**F** and **G**) Hematoxylin, eosin and alcian blue-stained horizontal sections of the lower thoracic spine at P11 (F) and P3 (G). (F) No acceleration of synchondrosis closure in Fgfr3 G374R mice, in which the *Col1a1-Cre* transgene was used to recombine *Fgfr3* in osteoblasts. (G) Premature synchondrosis closure (arrows) in Fgfr3 G374R mice, in which the *Col2a1-Cre* transgene was used to recombine *Fgfr3* in chondrocytes.

Expression of Fgfr3 G374R in chondrocytes increases osteoblast differentiation in a paracrine fashion

Fgfr3 is strongly expressed in chondrocytes and also expressed in osteoblasts (31). To examine whether the increased osteoblast differentiation was caused by the increased Fgfr3 signaling in osteoblasts or chondrocytes, we expressed Fgfr3 G374R in osteoblasts and chondrocytes of the *Col1a1-LacZ* transgenic mice using the *Col1a1-Cre* and *Col2a1-Cre* transgenes, and osteoblasts were identified by X-gal staining (Fig. 5C and D and data not shown). The tissue specificity of Cre activity was confirmed by using the *ROSA26* reporter mice (Fig. 5E). *Fgfr3* mutant mice harboring the *Col2a1-Cre* transgene showed an increased number of X-gal-stained osteoblasts in the periosteum and at the chondro-osseous junction of synchondroses in the spine, sternum and cranial base (Fig. 5C and D and data not shown) at P3. These mice also showed a dwarf phenotype and premature synchondrosis closure (Fig. 5G and data not shown). In contrast, the use of *Col1a1-Cre* transgene did not result in an increased number of X-gal-stained osteoblasts (data not shown). These mice did not show premature synchondrosis closure and grew normally without obvious skeletal abnormalities (Fig. 5F and data not shown). These observations indicate Fgfr3 signaling in chondrocytes promotes osteoblast differentiation and bone formation around synchondroses in a paracrine fashion. A similar increase in osteoblasts

was also observed in the perichondrium of long bones when Fgfr3 G374R is expressed in chondrocytes using the *Col2a1-Cre* transgene (data not shown).

Premature synchondrosis closure in mice that express a constitutively active mutant of MEK1 (S218/222E, Δ32-51) in chondrocytes

To investigate downstream signaling that mediates premature synchondrosis closure, we examined synchondroses of *Col2a1-MEK1* transgenic mice that express a constitutively active mutant MEK1 in chondrocytes and show an achondroplasia-like dwarfism (32). Skeletal preparation of 11-day-old *Col2a1-MEK1* mice showed premature closure of multiple synchondroses including the cranial base, vertebrae, pelvis and hyoid (Fig. 6A and B and data not shown). These observations are consistent with increased MAPK signaling mediating the premature synchondrosis closure seen in the Fgfr3 mutants.

We also crossed *Fgfr3 G374R* mutant mice with transgenic mice that overexpress C-type natriuretic peptide (CNP) in chondrocytes, since CNP can inhibit the ERK MAPK pathway in chondrocytes (33,34). Transgenic overexpression of CNP mice partially rescued the premature synchondrosis closure in the sternum (Supplementary Material, Fig. S3). In contrast, loss of Stat1, another downstream signaling molecule of Fgfr3, did not rescue the premature closure of the synchondroses (Supplementary Material, Fig. S4) (35,36). These observations further support the notion that increased *Fgfr3* signaling accelerates synchondrosis closure through the MAPK pathway.

Increased bone formation in mice that express a constitutively active mutant of MEK1 (S218/222E, Δ32-51) in chondrocytes

Consistent with the notion that increased Fgfr3 signaling in chondrocytes leads to increased osteoblast differentiation, and the MAPK pathway mediates Fgfr3 signaling, we found an increased bone formation in *Col2a1-MEK1* mice. In this mouse model, the transgene harbors an *IRES-LacZ* cassette, and no osteoblast expression of the transgene was detected by X-gal staining. While no cortical bone was observed over the spheno-occipital synchondrosis of wild-type mice at P1, the cortical bone over the spheno-occipital synchondrosis already connected the cortices of the sphenoid and occipital bones in *Col2a1-MEK1* mice, indicating accelerated cortical bone formation (Fig. 6C upper panels). This accelerated bone formation was further confirmed by *in situ* hybridization for an osteoblast marker *bone sialoprotein* (*BSP*) (Fig. 6C lower panels). These observations indicate that increased MEK1 signaling in chondrocytes stimulates bone formation over the synchondrosis and suggest that an increased bone formation in Fgfr3 G374R mice is mediated by increased MAPK signaling in chondrocytes.

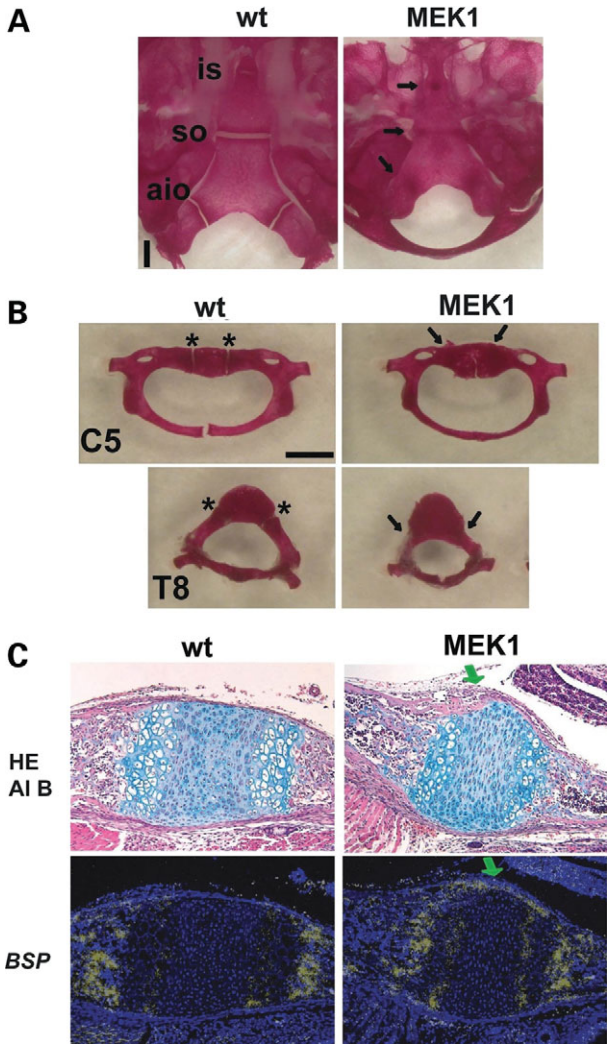

Figure 6. Premature synchondrosis closure in mice that express a constitutively active mutant of MEK1 (S218/222E, Δ32-51) in chondrocytes. Skeletal preparations of the (**A**) cranial base and (**B**) spine showed premature synchondrosis closure. Arrows indicate fused synchondroses. Abbreviations: is, intersphenoid; so, spheno-occipital; aio, anterior intraoccipital; asterisk, neurocentral synchondroses; C5, fifth cervical vertebrae; T8, eighth thoracic vertebrae. (**C**) Upper panels show hematoxylin, eosin and alcian blue (HE Al B) staining of the spheno-occipital synchondrosis at P1. In transgenic mice that express a constitutively active mutant of MEK1 in chondrocytes, the eosin-stained bone cortex (green arrow) over the synchondrosis connects the cortices of the sphenoid and occipital bones, whereas in wild type mice, the synchondrosis is flanked by the thin perichondrium. Lower panels show *in situ* hybridization for *Bone sialoprotein* (*BSP*) of neighboring sections. While the perichondrium flanking the synchondrosis did not express *Bone sialoprotein* in wild type mice, mice that express a constitutively active mutant of MEK1 in chondrocytes showed intense signal for *Bone sialoprotein* over the synchondrosis (green arrow), indicating accelerated osteoblast differentiation in the perichondrium.

Regulation of Bmp-2, Bmp-7, Noggin, Chordin, Gremlin by FGF18 and the MAPK pathway in primary chondrocytes

Because our data indicate that Fgfr3 signaling in chondrocytes regulates osteoblast differentiation, and the regulation is likely to be mediated by the MAPK pathway, we looked for downstream targets that are regulated by FGF18 in an MAPK-dependent manner by microarray analyses (Supplementary Material, Table S1). FGF18 is a putative physiological ligand for Fgfr3 (37,38). Among genes that were differentially regulated by FGF18 in primary chondrocytes, we consistently found a number of Bmp ligands and Bmp antagonists. The gene

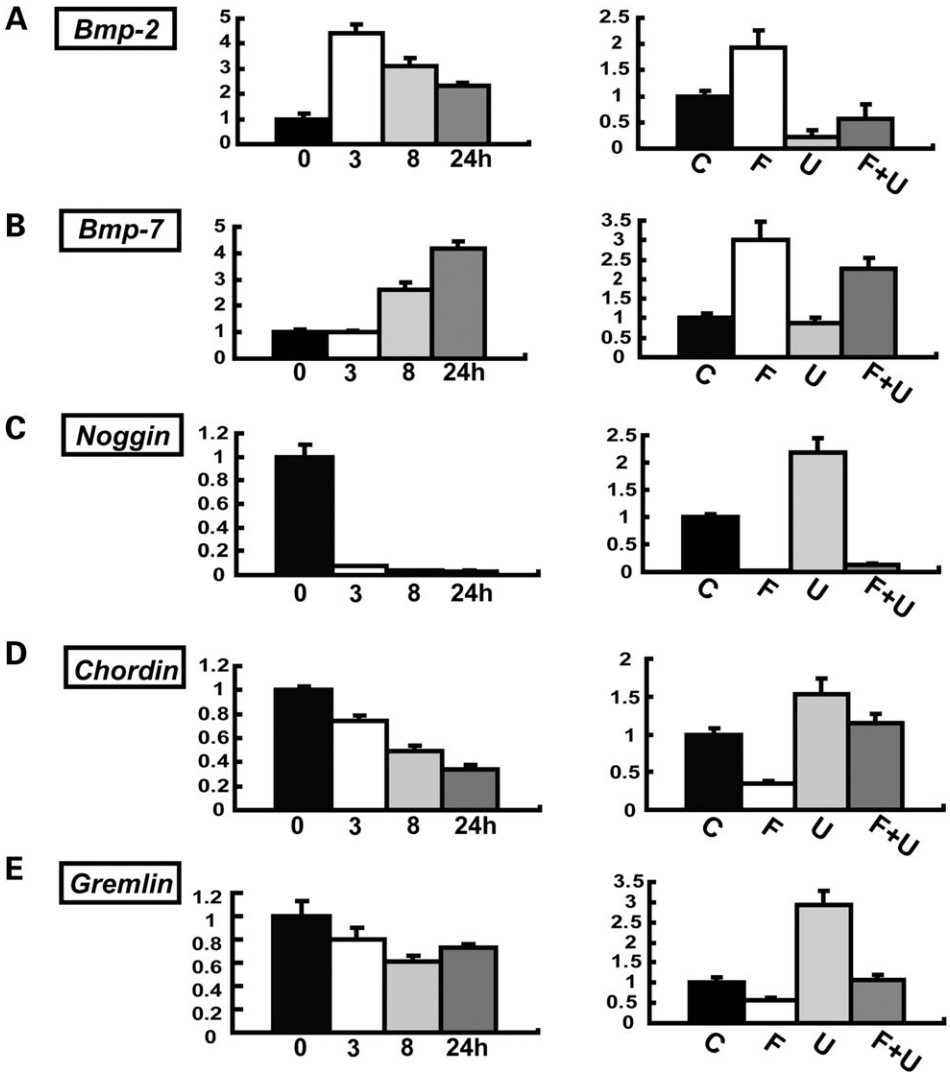

Figure 7. FGF18 upregulates *Bmp-2, Bmp-7* and downregulates *Noggin, Chordin* and *Gremlin* in primary chondrocytes. (**A**) *Bmp-2*, (**B**) *Bmp-7*, (**C**) *Noggin*, (**D**) *Chordin* and (**E**) *Gremlin*. For each gene, the left panel shows the time course of gene expression levels after stimulation with 20 ng/ml FGF18. Total RNA was extracted at 3, 8 and 24 h after stimulation. mRNA expression levels were examined by real-time PCR. The right panel shows the effects of U0126 on gene expression. Primary chondrocytes were treated with 20 ng/ml FGF18 in the presence or absence of 20 μM U0126. (C) Control, (F) FGF18, (U) U0126, (F + U) FGF18 and U0126. Total RNA was extracted at 3 h after FGF18 stimulation for *Bmp-2* and at 24 h for *Bmp-7*, *Noggin*, *Chordin* and *Gremlin*. In all panels, mRNA levels were normalized by the values for the control culture harvested at each time point. Data represent mean ± SD. The figure presents data from one of two experiments that produced similar results.

regulation of Bmp ligands and Bmp antagonists was further confirmed by real-time PCR in primary chondrocytes. Primary chondrocytes were treated with FGF18 in the presence or absence of U0126, and RNA was extracted at 3, 8 and 24 h after treatment. We found that FGF18 upregulates both *Bmp-2* and *Bmp-7* about 4-fold in a time-dependent manner (Fig. 7A and B, left). The upregulation of *Bmp-2* and *Bmp-7* by FGF18 was at least partially inhibited by U0126 (Fig. 7A and B, right). We next examined the expression of Bmp antagonists, *Noggin*, *Chordin* and *Gremlin*. FGF18 inhibited, while U0126 upregulated, all three Bmp antagonists although with different kinetics and different magnitude (Fig. 7C–E). The inhibition of *Noggin, Chordin* and *Gremlin* expression by FGF18 was at least partially inhibited by U0126, suggesting that the regulation was mediated by the ERK MAPK pathway. The MAPK regulation of *Bmp2, Bmp7, Noggin* and *Gremlin* was further confirmed by infecting primary chondrocytes with adenovirus expressing a constitutively active mutant MEK1 S217/221E (Supplementary Material, Fig. S5). Collectively, these observations indicate that FGF18 upregulates *Bmp-2*, *-7*, and downregulates *Noggin*, *Chordin* and *Gremlin* in primary chondrocytes, and the MAPK pathway plays a central role in the regulation.

Decreased *Noggin* and *Gremlin* expression and increased *Bmp-7* expression in chondrocytes of mice that express Fgfr3 G374R

We further examined the expression of Bmp ligands and Bmp antagonists in the synchondroses of $Fgfr3^{G374R/+}$ mice and *Col2a1-MEK1* mice by *in situ* hybridization.

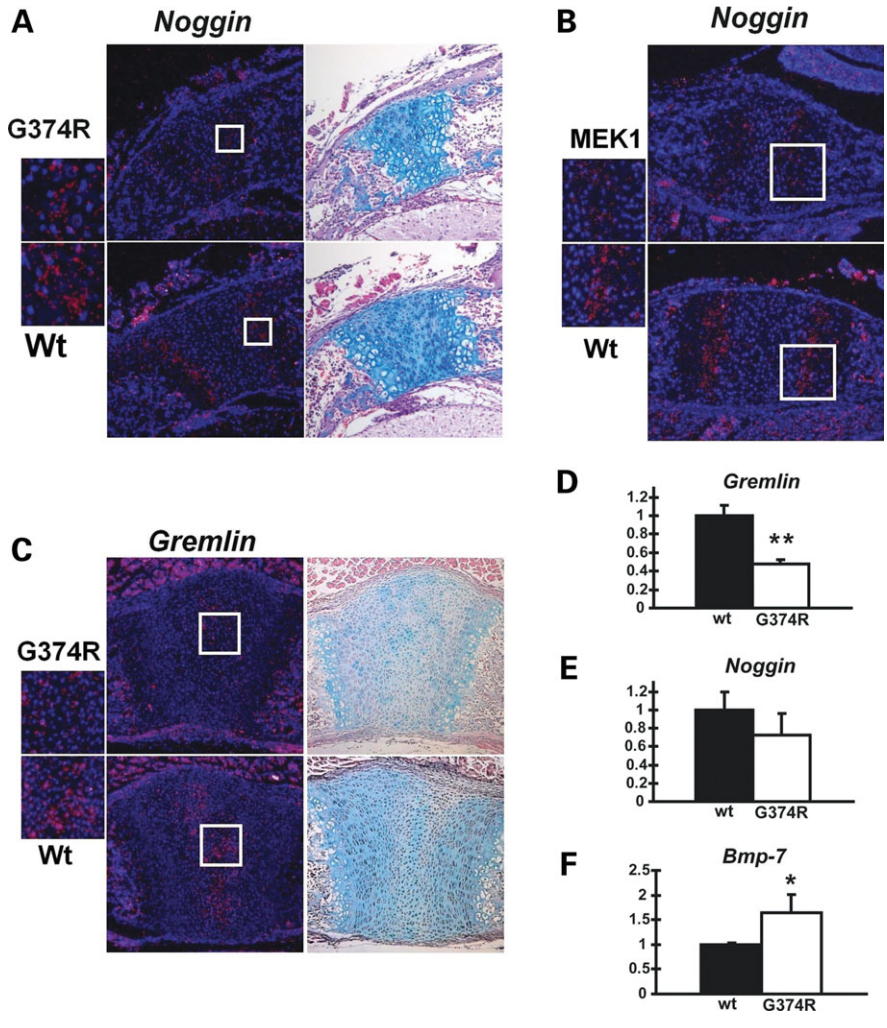

Figure 8. Decreased *Noggin* and *Gremlin* expression in chondrocytes of mice that express Fgfr3 G374R. (**A**) *In situ* hybridization analysis showed reduced *Noggin* expression in the neurocentral synchondroses in the lower thoracic spine of mice that express Fgfr3 G374R at P1. The boxed area is magnified on the left. Neighboring sections were stained with alcian blue. (**B**) *In situ* hybridization analysis showed decreased *Noggin* expression in the spheno-occipital synchondrosis of mice that express a constitutively active mutant MEK1(S218/222E, Δ32-51) in chondrocytes compared with wild-type littermate mice at P1. Alcian blue staining of the neighboring sections are presented in Fig. 6C. (**C**) *In situ* hybridization analysis showed reduced *Gremlin* expression in the synchondroses in the sternum of mice that express Fgfr3 G374R at P1. Neighboring sections were stained with alcian blue staining. (**D**–**F**) Real-time PCR analysis showed reduced *Gremlin* (D) and *Noggin* (E) expression and increased *Bmp-7* (F) expression in the epiphyseal cartilage of mice that express Fgfr3 G374R ($n = 3$) compared with wild-type littermate mice ($n = 3$) at P3. Total RNA was extracted from the epiphyseal cartilage of long bones. The expression of each gene was normalized by the expression level in wild type mice. Data represent mean ± SD. The figure presents representative data from repeated experiments. $^{*}P < 0.05$, $^{**}P < 0.02$ (unpaired Student's *t*-test).

In situ hybridization analysis was done at P1, when the growth plate-like architecture is still maintained in the synchondroses. We found that *Noggin* is expressed in the prehypertrophic zone of the synchondrosis, whereas *Gremlin* is expressed in the resting zone (Figs 8A–C and 9). The expression level and expression domain of *Noggin* were decreased in the synchondroses of *Fgfr3*$^{G374R/+}$ mice and *Col2a1-MEK1* mice compared with wild-type mice (Fig. 8A and B). Similarly, *Gremlin* expression was decreased in *Fgfr3*$^{G374R/+}$ mice compared with wild-type mice (Fig. 8C). Unlike FGF18-treated primary chondrocytes, we did not observe an obvious difference in *Bmp-2* and *Bmp-7* expression in these mice in *in situ* hybridization (data not shown). This difference might be due to the long-term Fgfr3 stimulation *in vivo* and short-term stimulation *in vitro*.

We next examined *Noggin*, *Gremlin*, *Chordin*, *Bmp-2* and *Bmp-7* expression in the epiphyseal cartilage of long bones by real-time PCR. RNA was directly extracted from the epiphyseal cartilage of *Fgfr3*$^{G374R/+}$ mice and wild-type littermate mice. Consistent with the *in situ* hybridization analysis of the synchondrosis, there was a statistically significant decrease in *Gremlin* expression in the epiphyseal cartilage of *Fgfr3*$^{G374R/+}$ mice compared with wild-type mice (Fig. 8D). Real-time PCR analysis also showed a modest decrease in *Noggin* expression; however, this did not reach statistical significance (Fig. 8E). In contrast, *Bmp-7* expression was consistently increased in the epiphyseal cartilage of *Fgfr3*$^{G374R/+}$ mice (Fig. 8F). *Chordin* and *Bmp-2* did not show an obvious difference between *Fgfr3*$^{G374R/+}$ mice and wild-type littermate mice (data not shown). Altogether, these observations

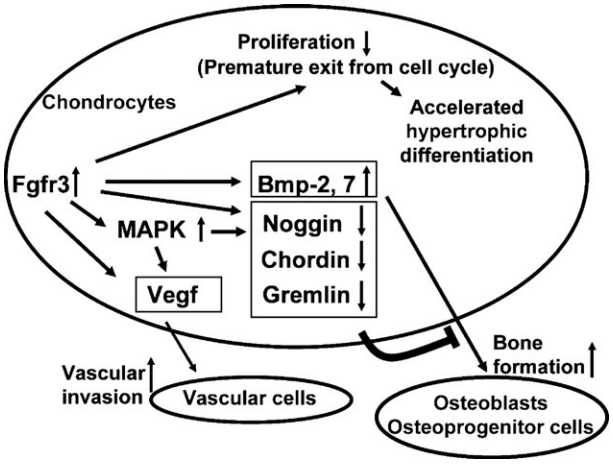

Figure 9. Model whereby increased Fgfr3 signaling in chondrocytes causes premature synchondrosis closure and unification of ossification centers. Increased Fgfr3 signaling induces premature exit from the cell cycle and accelerates the transition into hypertrophic chondrocytes. Increased Fgfr3 signaling also causes upregulation of Vegf in chondrocytes, promoting vascular invasion. Increased secretion of Bmp ligands and decreased secretion of Bmp antagonists result in enhanced osteoblast differentiation of osteoprogenitors in the periosteum, promoting bone formation and fusion of ossification centers. The upregulation of Vegf and Bmps and downregulation of Bmp antagonists are at least partially mediated by the MAPK pathway.

suggest that increased Fgfr3 and ERK MAPK signaling in chondrocytes causes decreased expression of BMP antagonists, which in turn could affect chondrocyte phenotype of the closing synchondroses and osteoblast differentiation in the adjacent perichondrium.

DISCUSSION

In this study, we demonstrated premature synchondrosis closure and fusion of ossification centers in the spine and cranial base in one case of homozygous achondroplasia with the G380R mutation and four cases of thanatophoric dysplasia with the R248C and stop codon mutations. We also found that multiple synchondroses close prematurely in mice that express Fgfr3 G374R, which corresponds to the human achondroplasia mutation G380R. The premature closure of synchondroses may account for the stenosis of the foramen magnum and spinal canals in patients with achondroplasia. If this is the case, then any growth-promoting treatment for these complications of achondroplasia must precede the timing of the synchondrosis closure. In addition to recognizing that FGFR3 mutations contribute to premature closure of synchondroses, it is also essential to understand the mechanism by which this occurs.

Activation of Fgfr3 signaling in chondrocytes causes premature synchondrosis closure

Although premature synchondrosis closure in the cranial base has also been reported in mice harboring mutations Fgfr3 G369C and G365C (39,40), the precise mechanisms of accelerated closure remain unknown. The advanced osteogenesis was also noted in these studies, however, whether the premature synchondrosis closure is primarily caused by aberrant chondrogenesis or advanced osteogenesis remain unresolved. In this study, we clearly demonstrated that premature synchondrosis closure is caused by increased Fgfr3 signaling in chondrocytes. The premature synchondrosis closure in the Fgfr3 G374R mice was associated with premature loss of proliferating chondrocytes, increased vascular invasion and increased bone formation. Chondrocyte proliferation in the synchondrosis is essential for the maintenance of the synchondrosis, since hypertrophic chondrocytes of the synchondrosis are continuously removed at the chondro-osseous junction on both sides. Increased vascular invasion would also accelerate synchondrosis closure, while increased bone formation would accelerate the fusion of ossification centers.

Fgfr3 signaling in chondrocytes regulates osteoblast differentiation in a paracrine fashion

Our genetic experiments further indicated that Fgfr3 signaling in chondrocytes, not in osteoblasts, regulates osteoblast differentiation in a paracrine fashion. Regulatory sequences of *Col2a1* have been reported to drive transgene expression in some of the periosteal cells and osteoblasts, raising the possibility that Fgfr3 G374R expressed in osteoblasts promotes osteoblast differentiation (41). However, several lines of evidence strongly argue against this possibility. First, as shown in Fig 5E, no recombination in osteoblasts was detected using the *Col2a1-Cre* mouse line. Secondly, recombination of the *Fgfr3* allele in osteoblasts using the *Col1a1-Cre* transgene did not promote osteoblast differentiation surrounding the synchondrosis. Third, the *Col2a1-MEK1* transgenic mice that express the transgene in chondrocytes but not in osteoblasts show accelerated osteoblast differentiation surrounding the synchondrosis. Altogether, these observations indicate that Fgfr3 signaling in chondrocytes coordinately regulates synchondrosis closure by regulating osteoblast differentiation and bone formation in a paracrine fashion.

In the human thanatophoric dysplasia specimens, we observed bony overgrowth on both sides of a synchondrosis. The bony overgrowth meets on the sides and fuses, leading to a loss of the synchondrosis. This bony overgrowth is similar to the lateral overgrowth of metaphyseal bone around the physis in the long bones of thanatophoric dysplasia and achondroplasia (42). The identification of secreted molecules from chondrocytes that mediate the increased bone formation would provide additional targets for controlling synchondrosis closure in thanatophoric dysplasia and achondroplasia.

Among cytokines and growth factors expressed in chondrocytes, *Indian hedgehog (Ihh)* has been implicated in the bone formation in the periosteum (43). However, Ihh is unlikely to be the mediator of Fgfr3 signaling for bone formation, since our *in situ* hybridization analysis showed that *Ihh* expression in the synchondroses of $Fgfr3^{G374R/+}$ mice and *Col2a1-MEK1* transgenic mice was indistinguishable from wild-type littermate mice in both mouse models (data not shown). In addition, Ihh has been shown to be downregulated in other mouse models expressing achondroplasia and thanatophoric dysplasia Fgfr3 mutants (44,45).

Increased Fgfr3 signaling inhibits expression of Bmp antagonists

Our *in vivo* and *in vitro* experiments identified Bmp ligands and Bmp antagonists as downstream targets of FGF signaling in chondrocytes. BMPs, such as Bmp-2 and Bmp-7, are strongly osteogenic, while their availability to the Bmp receptors is counterbalanced by BMP antagonists, such as Noggin, Gremlin and Chordin (46). Because BMP enhances chondrocyte hypertrophy (47), it is possible that increased BMP signaling together with increased FGF signaling in chondrocytes accelerated synchondrosis closure in *Fgfr3*$^{G374R/+}$ mice. In addition, increased availability of BMPs may have accelerated osteoblast differentiation in the adjacent perichondrium. Such paracrine regulation has been reported in the cranial suture where increased Fgfr2 signaling inhibits *Noggin* expression in the dura mater, which in turn promotes cranial suture closure (48). Consistent with this notion, our immunohistochemical analysis showed phosphorylation of Smad1, 5 and 8 in the perichondrium surrounding the synchondrosis, indicating the presence of BMP signaling (data not shown). However, we did not observe an obvious difference in the staining for phosphorylated-Smad1, 5 and 8 between wild-type and *Fgfr3*$^{G374R/+}$ mice, although immunohistochemistry may not be quantitative enough to detect a subtle difference. Nevertheless, our *in vivo* and *in vitro* data are consistent with the notion that Bmp ligands and Bmp antagonists are among the secreted mediators of Fgfr3 signaling in chondrocytes that regulate osteoblast differentiation.

Premature synchondrosis closure is mediated by the MAPK pathway

The identification of downstream pathways that mediate premature synchondrosis closure would provide therapeutic targets for preventing premature closure. Fgfr3 signaling is transduced to multiple signaling pathways, including Stat1, Stat3, Stat5, ERK1, ERK2, p38, phosopholipase C gamma, protein kinase C, Src, phosphatidylinositol 3-kinase, Akt and Pyk2 (35,36,45,49–51). Among these, at least Stat1 and the ERK MAPK pathway have been implicated in the regulation of skeletal development by Fgfr3 (32,35,36). In this study, we showed evidence that the MAPK pathway in chondrocytes plays a central role in premature synchondrosis closure and increased bone formation. *Col2a1-MEK1* transgenic mice showed accelerated synchondrosis closure similar to *Fgfr3*$^{G374R/+}$ mice, while loss of *Stat1* did not rescue the premature synchondrosis closure in *Fgfr3*$^{G374R/+}$ mice. Furthermore, overexpression in chondrocytes of CNP that is capable of inhibiting the MAPK pathway partially rescued the premature synchondrosis closure. The pharmacological inhibition of the MAPK pathway or activation of CNP signaling may prevent premature closure of synchondroses.

In summary, we found premature synchondrosis closure and increased bone formation in human samples of homozygous achondroplasia and thanatophoric dysplasia and in mouse models of achondroplasia. Our genetic experiments in mice indicated that Fgfr3 signaling in chondrocytes regulates osteoblast differentiation and bone formation in a paracrine fashion. Furthermore, *in vitro* and *in vivo* analyses suggested a role for Bmp signaling in the increased bone formation surrounding the synchondroses. On the basis of these observations, we propose that Fgfr3 in chondrocytes coordinately regulates synchondrosis closure, bone formation and unification of ossification centers. Spinal canal stenosis, foramen magnum stenosis and cranial base hypoplasia in human heterozygous achondroplasia patients may be caused by the premature closure of synchondroses. The timing of the closure of each synchondrosis should be examined in these patients, and the future growth-promoting treatment on the spine and cranial base must start before synchondrosis closure. Further analysis of the roles of Fgfr3 in chondrocytes may lead to new therapeutic approaches for preventing premature synchondrosis and growth plate closure in achondroplasia and other skeletal disorders.

MATERIALS AND METHODS

Human specimens

Human thanatophoric dysplasia and homozygous achondroplasia specimens were examined at the International Skeletal Dysplasia Registry at Cedar Sinai Medical Center. Synchondroses in the cranial base and lumbar vertebrae were first examined by X-ray and further processed for histological analysis. The formalin-fixed, undecalcified tissue was embedded in methylmethacrylate, sectioned with a tungsten blade and stained with Goldner's stain.

Mice

The institutional animal care and use committee of Case Western Reserve University approved all animal procedures. All animal care and use were performed in accordance with the institutional animal use methods and policies. Mice harboring the *Fgfr3 G374R* mutation that corresponds to the human achondroplasia mutation *G380R* and transgenic mice that express in chondrocytes a constitutively active mutant of MEK1 under the control of regulatory sequences of *Col2a1* were described previously (27,32). *Zp3-Cre* transgenic mice that express Cre recombinase in oocytes (52), *Prx1-Cre* transgenic mice that express Cre recombinase in all mesenchymal cells of the developing limb bud and sternum (53), *Col2a1-Cre* transgenic mice that express Cre recombinase in chondrocytes (54) and *Col1a1-Cre* transgenic mice that express Cre recombinase in osteoblasts (55) were used to delete the neomycin cassette in *Fgfr3*. Mice that express *LacZ* under the control of a 2.3 kb *Col1a1* osteoblast-specific promoter (28) were a generous gift from Dr. Benoit de Crombrugghe (U.T.M.D. Anderson Cancer Center, Houston, TX, USA). Transgenic mice that overexpress human *CNP* under the control of regulatory sequences of *Col2a1* were generated at the Transgenic Core Facility at Case Western Reserve University. The transgenic expression vector containing the promoter and enhancer sequences of mouse *Col2a1* was generously provided by Dr. Yoshihiko Yamada (National Institutes of Health, Bethesda, MD, USA). *Stat1*-null mice were purchased from Taconic (56). The *Fgfr3* allele was recombined using the *Zp3-Cre* transgene to express Fgfr3 G374R in the *Stat1*-null background (32).

Skeletal preparations

Mice were euthanized by carbon dioxide inhalation. After removing the skin, the whole body was fixed in 95% ethanol and stained with Alcian blue and Alizarin Red S. Soft tissues were removed with KOH treatment.

Histological examination

Tissues were fixed in 4% formaldehyde in phosphate-buffered saline (PBS) for 20–24 h at 4°C and embedded in paraffin. Postnatal tissues were demineralized in 0.5 M EDTA before embedding. Sections were cut in 7 μm and stained with hematoxylin, eosin and alcian blue. For immunostaining, endogenous peroxidase activity was quenched with 3% hydrogen peroxidase. Heat-induced epitope retrieval was performed in Borgdecloaker (Biocare) using a pressure cooker (Biocare). Primary antibodies for von Willebrand factor (Chemicon, CA, USA), Runx2 (Santa Cruz Biotechnology Inc.) and Osteopontin (R&D) were applied onto each section and incubated at room temperature for 1 h or at 4°C overnight. After washing with PBS-containing 0.01% Triton X, sections were incubated with an anti-rabbit or anti-goat peroxidase-conjugated polymer (Super PicTure Polymer Detection kit, Zymed, CA, USA). Immunostaining of type X collagen was done using a mouse anti-type X collagen antibody (Clone X53, Cat. No. 2031501005, quartett Immunodiagnostika&Biotechnologie GmbH, Berlin, Germany) and MM biotinylation kit (Biocare medical, CA, USA). Color was developed using diaminobenbenzidine or 3,3′,5,5′-tetramethylbenzidine (KPL Inc., MD, USA). Sections were counterstained with Orcein or Contrast green (KPL). For cell proliferation analysis, BrdU (Zymed) was injected intraperitoneally or subcutaneously at a dose of 300 μg/kg. Mice were sacrificed 2 h after injection. BrdU-labeled cells were identified using BrdU-staining kit (Zymed). For X-gal staining, tissues were fixed with 2% formalin in PBS, washed in rinse buffer (0.1% sodium deoxycholate, 0.2% NP40, 2 mM $MgCl_2$, 0.1 M phosphate buffer, pH 7.3), and stained in X-gal solution (1 mg/ml X-gal, 5 mM ferricyanide, 5 mM ferrocyanide in the rinse buffer). Images were taken with Leica microscope using Leica suite software.

In situ hybridization

Slides were deparaffinized and fixed in 4% formaldehyde. Sections were then digested with proteinase K (1 μg/ml) for 20 min at 37°C, and acetylated in 0.25% acetic anhydride in 0.1 M triethanolamine-hydrochloride. After re-fixation in 4% formaldehyde, sections were hybridized with ^{35}S-labeled antisense riboprobes in hybridization buffer (50% deionized formamide, 300 mM NaCl, 20 mM Tris–HCl, pH 8.0, 5 mM EDTA, 0.5 mg/ml yeast tRNA, 10% dextran sulfate, and 1× Denhardt's) in a humidified chamber at 55°C overnight. After hybridization, slides were washed with 5× SSC at 50°C, 50% formamide, 2× SSC at 65°C and 1× NTE (0.5 M NaCl, 10 mM Tris–HCl, pH 8.0, 5 mM EDTA) at 37°C then treated with RNase A (20 μg/ml) and RNase T1 (1 U/μl) in 1× NTE at 37°C for 20 min. Slides were further washed in 1× NTE at 37°C, 50% formamide, 2× SSC at 65°C, 2× SSC, 0.1× SSC, and then dehydrated with graded concentrations of ammonium acetate and ethanol. Slides were dipped in NTB emulsion (Kodak) and exposed for 5 days to 2 weeks. Slides were then developed and counterstained with Hoechst 33258 (Sigma).

Cell cultures

Mouse costal chondrocytes were isolated from 3- or 4-day-old B6D2 (C57BL6/DBA2) wild-type mice (57). The rib cages were first digested with 3 mg/ml collagenase at 37°C for about 1 h to remove soft tissues. Chondrocytes were isolated from the ribs by further digesting with 0.5 mg/ml collagenase overnight in a CO_2 incubator at 37°C. For FGF18 and U0126 treatment, cells were plated either in 60 mm dishes, 12-well plates or 24-well plates at a density of 1×10^5 cells/cm^2, cultured in high-glucose Dulbecco's Modified Eagle Medium (Invitrogen) supplemented with L-glutamine 2 mM (Invitrogen), penicillin (50 units/ml), streptomycin (50 μg/ml) and 10% FBS for 3 days until reaching subconfluence, and treated with 20 ng/ml FGF18 (R&D) in the presence or absence of 20 μM U0126 (Promega, Madison, WI, USA). Total RNA was extracted at 3, 8 and 24 h after the stimulation using RNeasy kit (Qiagen, Valencia, CA, USA). For adenovirus infection, primary chondrocytes were plated in 12-well plates at 2×10^5 cells/cm^2. Cells were infected with adenovirus encoding a constitutively active MEK1 S217/221E or empty control adenovirus (Cell Biolabs, San Diego, CA, USA) at an MOI of 100 one-h after plating. RNA was harvested 48 h after adenovirus infection.

Isolation of RNA from epiphyseal cartilage

For direct RNA extraction from the epiphyseal cartilage, the epiphyses in the proximal tibia, distal femur and distal humerus were collected from 3-day-old mice under the dissecting microscope. Harvested epiphyses were homogenized in RLT solution (Qiagen) using Power Gen 500 (Fisher, Pittsburgh, PA, USA). Total RNA was extracted using RNeasy kit (Qiagen).

Real-time PCR

RNA was reverse-transcribed to cDNA with High Capacity cDNA Archive Kit (Applied Biosystems). Real-time PCR was performed on the Applied Biosystems 7500 real-time PCR detection system. TaqMan probe sets were designed and synthesized by Applied Biosystems (*Bmp-2*; Mm01962382_s1, *Bmp-7*; Mm00432105_m1, *Noggin*; Mm01297833_s1, *Chordin*; Mm00438203_m1, *Gremlin 1*; Mm00488615_s1, *Gapdh*; 4352932E). To compare gene expression levels, the comparative cycle threshold (Ct) method was used. *Gapdh* was used as an endogenous control to correct for potential variation in RNA loading or in efficiency of amplification.

Microarray analysis

Microarray analysis was performed in the Gene Expression and Genotyping Facility of the Case Comprehensive Cancer Center at Case Western Reserve University. Briefly, total RNA was cleaned up with Qiagen spin columns and converted

into double-stranded cDNA. cDNA was labeled with biotin and fragmented according to the manufacturer's protocol. The fragmented cRNA was hybridized onto Affymetrix mouse 4.30 chips. Data analysis was done using the Affymetrix GCOS software.

SUPPLEMENTARY MATERIAL

Supplementary Material is available at *HMG* Online.

ACKNOWLEDGEMENTS

We thank Chu-Xia Deng (National Institutes of Health, Bethesda, MD, USA), Tamayuki Shinomura (Tokyo Medical and Dental University, Tokyo, Japan), Céline Colnot (University of California at San Francisco, CA, USA), Richard Harland (University of California at Berkeley, CA, USA), Yasuhide Furuta (U.T.M.D. Anderson Cancer Center, Houston, TX, USA), Andrew McMahon (Harvard University, Cambridge, MA, USA), Jinkun Chen (U.T Health Science Center at San Antonio, TX, USA) for probes, Yoshihiko Yamada (National Institutes of Health, Bethesda, MD, USA) for the transgenic expression vector, James Martin (Institute of Biosciences and Technology, Houston, TX, USA) and Benoit de Crombrugghe (U.T.M.D. Anderson Cancer Center) for *Prx1-Cre* and *Col1a1-LacZ* transgenic mice. We are grateful to Dr. Masahiro Kurosaka (Kobe University) for his continuous support for this work. We also thank Drs. Guang Zhou and Douglas Armstrong for scientific discussion and Ms. Valerie Schmedlen for editorial assistance.

Conflict of Interest statement. None declared.

FUNDING

This work was supported by Arthritis Investigator Award of the Arthritis Foundation, March of Dimes Birth Defects Foundation [grant number #6-FY06-341], National Institutes of Health [grant number R21DE017406] to S.M., National Institutes of Health [grant number 5P01-HD22657, M01-RR00425], and Winnick family research scholar's award to W.R.W, Arthritis National Research Foundation and National Institutes of Health [grant number 5K08AR53943-2] to H.B., the Howard Hughes Medical Institute to M.L.W. The Gene Expression and Genotyping Facility of the Case Comprehensive Cancer Center was supported by National Institutes of Health [grant number P30 CA43703].

REFERENCES

1. van der Eerden, B.C., Karperien, M. and Wit, J.M. (2003) Systemic and local regulation of the growth plate. *Endocr. Rev.*, **24**, 782–801.
2. Nilsson, O., Marino, R., De Luca, F., Phillip, M. and Baron, J. (2005) Endocrine regulation of the growth plate. *Horm. Res.*, **64**, 157–165.
3. Peters, K., Ornitz, D., Werner, S. and Williams, L. (1993) Unique expression pattern of the FGF receptor 3 gene during mouse organogenesis. *Dev. Biol.*, **155**, 423–430.
4. Delezoide, A.L., Benoist-Lasselin, C., Legeai-Mallet, L., Le Merrer, M., Munnich, A., Vekemans, M. and Bonaventure, J. (1998) Spatio-temporal expression of FGFR 1, 2 and 3 genes during human embryo-fetal ossification. *Mech. Dev.*, **77**, 19–30.
5. Rousseau, F., Bonaventure, J., Legeai-Mallet, L., Pelet, A., Rozet, J.M., Maroteaux, P., Le Merrer, M. and Munnich, A. (1994) Mutations in the gene encoding fibroblast growth factor receptor-3 in achondroplasia. *Nature*, **371**, 252–254.
6. Rousseau, F., Saugier, P., Le Merrer, M., Munnich, A., Delezoide, A.L., Maroteaux, P., Bonaventure, J., Narcy, F. and Sanak, M. (1995) Stop codon FGFR3 mutations in thanatophoric dwarfism type 1. *Nat. Genet.*, **10**, 11–12.
7. Rousseau, F., el Ghouzzi, V., Delezoide, A.L., Legeai-Mallet, L., Le Merrer, M., Munnich, A. and Bonaventure, J. (1996) Missense FGFR3 mutations create cysteine residues in thanatophoric dwarfism type I (TD1). *Hum. Mol. Genet.*, **5**, 509–512.
8. Shiang, R., Thompson, L.M., Zhu, Y.Z., Church, D.M., Fielder, T.J., Bocian, M., Winokur, S.T. and Wasmuth, J.J. (1994) Mutations in the transmembrane domain of FGFR3 cause the most common genetic form of dwarfism, achondroplasia. *Cell*, **78**, 335–342.
9. Bellus, G.A., McIntosh, I., Smith, E.A., Aylsworth, A.S., Kaitila, I., Horton, W.A., Greenhaw, G.A., Hecht, J.T. and Francomano, C.A. (1995) A recurrent mutation in the tyrosine kinase domain of fibroblast growth factor receptor 3 causes hypochondroplasia. *Nat. Genet.*, **10**, 357–359.
10. Trotter, T.L. and Hall, J.G.the Committee on Genetics (2005) Health supervision for children with achondroplasia. *Pediatrics*, **116**, 771–783.
11. Horton, W.A., Hall, J.G. and Hecht, J.T. (2007) Achondroplasia. *Lancet*, **370**, 162–172.
12. Pauli, R.M., Scott, C.I., Wassman, E.R. Jr, Gilbert, E.F., Leavitt, L.A., Ver Hoeve, J., Hall, J.G., Partington, M.W., Jones, K.L., Sommer, A. *et al.* (1984) Apnea and sudden unexpected death in infants with achondroplasia. *J. Pediatr.*, **104**, 342–348.
13. Hecht, J.T., Francomano, C.A., Horton, W.A. and Annegers, J.F. (1987) Mortality in achondroplasia. *Am. J. Hum. Genet.*, **41**, 454–464.
14. Hecht, J.T. and Butler, I.J. (1990) Neurologic morbidity associated with achondroplasia. *J. Child Neurol.*, **5**, 84–97.
15. Danielpour, M., Wilcox, W.R., Alanay, Y., Pressman, B.D. and Rimoin, D.L. (2007) Dynamic cervicomedullary cord compression and alterations in cerebrospinal fluid dynamics in children with achondroplasia. Report of four cases. *J. Neurosurg.*, **107**, 504–507.
16. Rimoin, D.L. (1995) Cervicomedullary junction compression in infants with achondroplasia: when to perform neurosurgical decompression. *Am. J. Hum. Genet.*, **56**, 824–827.
17. Hecht, J.T., Horton, W.A., Reid, C.S., Pyeritz, R.E. and Chakraborty, R. (1989) Growth of the foramen magnum in achondroplasia. *Am. J. Med. Genet.*, **32**, 528–535.
18. Soames, R.W. (1995) *Gray's Anatomy. The Anatomical Basis of Medicine and Surgery*. 38th edn. Churchill Livingstone, New York, pp. 547–613.
19. Madeline, L.A. and Elster, A.D. (1995) Suture closure in the human chondrocranium: CT assessment. *Radiology*, **196**, 747–756.
20. Okamoto, K., Ito, J., Tokiguchi, S. and Furusawa, T. (1996) High-resolution CT findings in the development of the sphenooccipital synchondrosis. *AJNR Am. J. Neuroradiol.*, **17**, 117–120.
21. Sahni, D., Jit, I., Neelam and Suri, S. (1998) Time of fusion of the basisphenoid with the basilar part of the occipital bone in northwest Indian subjects. *Forensic Sci. Int.*, **98**, 41–45.
22. Kahana, T., Birkby, W.H., Goldin, L. and Hiss, J. (2003) Estimation of age in adolescents –the basilar synchondrosis. *J. Forensic Sci.*, **48**, 504–508.
23. Maat, G.J., Matricali, B. and van Persijn van Meerten, E.L. (1996) Postnatal development and structure of the neurocentral junction. Its relevance for spinal surgery. *Spine.*, **21**, 661–666.
24. Rajwani, T., Rajwani, T., Bhargava, R., Moreau, M., Mahood, J., Raso, V.J., Jiang, H. and Bagnall, K.M. (2002) MRI characteristics of the neurocentral synchondrosis. *Pediatr. Radiol.*, **32**, 811–816.
25. Rajwani, T., Bhargava, R., Lambert, R., Moreau, M., Mahood, J., Raso, V.J., Jiang, H., Huang, E.M., Wang, X., Daniel, A. *et al.* (2002) Development of the neurocentral junction as seen on magnetic resonance images. *Stud. Health Technol. Inform.*, **91**, 229–234.
26. Hoshino (2004) A study of the postnatal development of vertebrae in medieval human bones. *St. Marianna Med. J.*, **32**, 551–559.
27. Wang, Y., Spatz, M.K., Kannan, K., Hayk, H., Avivi, A., Gorivodsky, M., Pines, M., Yayon, A., Lonai, P. and Givol, D. (1999) A mouse model for achondroplasia produced by targeting fibroblast growth factor receptor 3. *Proc. Natl Acad. Sci. USA*, **96**, 4455–4460.
28. Rossert, J., Eberspaecher, H. and de Crombrugghe, B. (1995) Separate cis-acting DNA elements of the mouse pro-alpha 1(I) collagen promoter

direct expression of reporter genes to different type I collagen-producing cells in transgenic mice. *J. Cell Biol.*, **129**, 1421–1432.
29. Komori, T., Yagi, H., Nomura, S., Yamaguchi, A., Sasaki, K., Deguchi, K., Shimizu, Y., Bronson, R.T., Gao, Y.H., Inada, M. *et al.* (1997) Targeted disruption of Cbfa1 results in a complete lack of bone formation owing to maturational arrest of osteoblasts. *Cell*, **89**, 755–764.
30. Otto, F., Thornell, A.P., Crompton, T., Denzel, A., Gilmour, K.C., Rosewell, I.R., Stamp, G.W., Beddington, R.S., Mundlos, S., Olsen, B.R. *et al.* (1997) Cbfa1, a candidate gene for cleidocranial dysplasia syndrome, is essential for osteoblast differentiation and bone development. *Cell*, **89**, 765–771.
31. Xiao, L., Naganawa, T., Obugunde, E., Gronowicz, G., Ornitz, D.M., Coffin, J.D. and Hurley, M.M. (2004) Stat1 controls postnatal bone formation by regulating fibroblast growth factor signaling in osteoblasts. *J. Biol. Chem.*, **279**, 27743–27752.
32. Murakami, S., Balmes, G., McKinney, S., Zhang, Z., Givol, D. and de Crombrugghe, B. (2004) Constitutive activation of MEK1 in chondrocytes causes Stat1-independent achondroplasia-like dwarfism and rescues the Fgfr3-deficient mouse phenotype. *Genes Dev.*, **18**, 290–305.
33. Yasoda, A., Komatsu, Y., Chusho, H., Miyazawa, T., Ozasa, A., Miura, M., Kurihara, T., Rogi, T., Tanaka, S., Suda, M. *et al.* (2004) Overexpression of CNP in chondrocytes rescues achondroplasia through a MAPK-dependent pathway. *Nat. Med.*, **10**, 80–86.
34. Krejci, P., Masri, B., Fontaine, V., Mekikian, P.B., Weis, M., Prats, H. and Wilcox, W.R. (2005) Interaction of fibroblast growth factor and C-natriuretic peptide signaling in regulation of chondrocyte proliferation and extracellular matrix homeostasis. *J. Cell Sci.*, **118**, 5089–5100.
35. Su, W.C., Kitagawa, M., Xue, N., Xie, B., Garofalo, S., Cho, J., Deng, C., Horton, W.A. and Fu, X.Y. (1997) Activation of Stat1 by mutant fibroblast growth-factor receptor in thanatophoric dysplasia type II dwarfism. *Nature*, **386**, 288–292.
36. Sahni, M., Ambrosetti, D.C., Mansukhani, A., Gertner, R., Levy, D. and Basilico, C. (1999) FGF signaling inhibits chondrocyte proliferation and regulates bone development through the STAT-1 pathway. *Genes Dev.*, **13**, 1361–1366.
37. Liu, Z., Xu, J., Colvin, J.S. and Ornitz, D.M. (2002) Coordination of chondrogenesis and osteogenesis by fibroblast growth factor 18. *Genes Dev.*, **16**, 859–869.
38. Ohbayashi, N., Shibayama, M., Kurotaki, Y., Imanishi, M., Fujimori, T., Itoh, N. and Takada, S. (2002) FGF18 is required for normal cell proliferation and differentiation during osteogenesis and chondrogenesis. *Genes Dev.*, **16**, 870–879.
39. Chen, L., Adar, R., Yang, X., Monsonego, E.O., Li, C., Hauschka, P.V., Yayon, A. and Deng, C.X. (1999) Gly369Cys mutation in mouse FGFR3 causes achondroplasia by affecting both chondrogenesis and osteogenesis. *J. Clin. Invest.*, **104**, 1517–1525.
40. Chen, L., Li, C., Qiao, W., Xu, X. and Deng, C. (2001) A Ser(365)–>Cys mutation of fibroblast growth factor receptor 3 in mouse downregulates Ihh/PTHrP signals and causes severe achondroplasia. *Hum. Mol. Genet.*, **10**, 457–465.
41. Sakai, K., Hiripi, L., Glumoff, V., Brandau, O., Eerola, R., Vuorio, E., Bösze, Z., Fässler, R. and Aszódi, A. (2001) Stage-and tissue-specific expression of a Col2a1-Cre fusion gene in transgenic mice. *Matrix Biol.*, **19**, 761–767.
42. Wilcox, W.R., Tavormina, P.L., Krakow, D., Kitoh, H., Lachman, R.S., Wasmuth, J.J., Thompson, L.M. and Rimoin, D.L. (1998) Molecular, radiologic, and histopathologic correlations in thanatophoric dysplasia. *Am. J. Med. Genet.*, **78**, 274–281.
43. St-Jacques, B., Hammerschmidt, M. and McMahon, A.P. (1999) Indian hedgehog signaling regulates proliferation and differentiation of chondrocytes and is essential for bone formation. *Genes Dev.*, **13**, 2072–2086.
44. Naski, M.C., Colvin, J.S., Coffin, J.D. and Ornitz, D.M. (1998) Repression of hedgehog signaling and BMP4 expression in growth plate cartilage by fibroblast growth factor receptor 3. *Development*, **125**, 4977–4988.
45. Li, C., Chen, L., Iwata, T., Kitagawa, M., Fu, X.Y. and Deng, C.X. (1999) A Lys644Glu substitution in fibroblast growth factor receptor 3 (FGFR3) causes dwarfism in mice by activation of STATs and ink4 cell cycle inhibitors. *Hum. Mol. Genet.*, **8**, 35–44.
46. Balemans, W. and Van Hul, W. (2002) Extracellular regulation of BMP signaling in vertebrates: a cocktail of modulators. *Dev. Biol.*, **250**, 231–250 (review).
47. Kobayashi, T., Soegiarto, D.W., Yang, Y., Lanske, B., Schipani, E., McMahon, A.P. and Kronenberg, H.M. (2005) Indian hedgehog stimulates periarticular chondrocyte differentiation to regulate growth plate length independently of PTHrP. *J. Clin. Invest.*, **115**, 1734–1742.
48. Warren, S.M., Brunet, L.J., Harland, R.M., Economides, A.N. and Longaker, M.T. (2003) The BMP antagonist noggin regulates cranial suture fusion. *Nature*, **422**, 625–629.
49. Hart, K.C., Robertson, S.C. and Donoghue, D.J. (2001) Identification of tyrosine residues in constitutively activated fibroblast growth factor receptor 3 involved in mitogenesis, Stat activation, and phosphatidylinositol 3-kinase activation. *Mol. Biol. Cell*, **12**, 931–942.
50. Meyer, A.N., Gastwirt, R.F., Schlaepfer, D.D. and Donoghue, D.J. (2004) The cytoplasmic tyrosine kinase Pyk2 as a novel effector of fibroblast growth factor receptor 3 activation. *J. Biol. Chem.*, **279**, 28450–28457.
51. Krejci, P., Masri, B., Salazar, L., Farrington-Rock, C., Prats, H., Thompson, L.M. and Wilcox, W.R. (2007) Bisindolylmaleimide I suppresses fibroblast growth factor-mediated activation of Erk MAP kinase in chondrocytes by preventing Shp2 association with the Frs2 and Gab1 adaptor proteins. *J. Biol. Chem.*, **282**, 2929–2936.
52. Lewandoski, M., Wassarman, K.M. and Martin, G.R. (1997) Zp3-cre, a transgenic mouse line for the activation or inactivation of loxP-flanked target genes specifically in the female germ line. *Curr. Biol*, **7**, 148–151.
53. Logan, M., Martin, J.F., Nagy, A., Lobe, C., Olson, E.N. and Tabin, C.J. (2002) Expression of Cre Recombinase in the developing mouse limb bud driven by a Prxl enhancer. *Genesis*, **33**, 77–80.
54. Ovchinnikov, D.A., Deng, J.M., Ogunrinu, G. and Behringer, R.R. (2000) Col2a1-directed expression of Cre recombinase in differentiating chondrocytes in transgenic mice. *Genesis*, **26**, 145–146.
55. Dacquin, R., Starbuck, M., Schinke, T. and Karsenty, G. (2002) Mouse alpha1(I)-collagen promoter is the best known promoter to drive efficient Cre recombinase expression in osteoblast. *Dev. Dyn.*, **224**, 245–251.
56. Meraz, M.A., White, J.M., Sheehan, K.C., Bach, E.A., Rodig, S.J., Dighe, A.S., Kaplan, D.H., Riley, J.K., Greenlund, A.C., Campbell, D. *et al.* (1996) Targeted disruption of the Stat1 gene in mice reveals unexpected physiologic specificity in the JAK-STAT signaling pathway. *Cell*, **84**, 431–442.
57. Lefebvre, V., Garofalo, S., Zhou, G., Metsäranta, M., Vuorio, E. and de Crombrugghe, B. (1994) Characterization of primary cultures of chondrocytes from type II collagen/beta-galactosidase transgenic mice. *Matrix Biol.*, **14**, 329–335.